Investigation and Fabrication of Brilliant Green Dye Material-Based Organic Heterojunction: Dielectric Response and Impedance Spectroscopy

M. Benhaliliba[1,*], Y.S. Ocak[2], A. Ayeshamariam[3] and C.E. Benouis[1]

[1]*Film Device Fabrication–Characterization and Application FDFCA Research Group USTOMB, 31130, Oran, Algeria*

[2]*Smart–Lab, 21280 Diyarbakir, Dicle University Turkey*

[3]*Department of Physics, Khadir Mohideen College, Adirampattinam – 614701, Thanjavur District, Tamil Nadu, India*

Abstract: Brilliant green (BG) dye material-based heterojunction is fabricated by a spin coating route and characterized by impedance analyzer. Here, we study the impedance spectroscopy of such organic material based thin film onto silicon substrate. The capacitance and conductance versus voltage (C-V), (G-V) characteristics are plotted. So, the dielectric response of BG based heterojunction is studied via the plotting of the dielectric constant, modulus components, complex impedance and Nyquist diagram. Real and imaginary parts of electrical conductivity are also plotted at several frequencies. Real and imaginary parts of electric modulus M'-V and M"-V are investigated for all experimental frequencies. The Z'-V characteristics of our device-based BG organic heterojunction exhibit a peak of 1383 Ω. It is confirmed that an anomalous peak of Z' is recorded within 0.5-1 V range. The drastic decay in Z"-V plot occurs for lower 100 and 200 kHz frequency range and Z" values become constant beyond 1V for all frequencies. Ac and Dc conductivity curves demonstrate a growth with frequency and angle phase approaches to 90º within reverse voltage. This result reveals a capacitive conduct of our device.

Keywords: Brilliant green, C-V curves, Dielectric response, G-V characteristics, Ac and Dc conductivity, Dielectric constants, Impedance spectroscopy.

1. INTRODUCTION

The development of a large number of synthetic and natural organic semiconductors, such as oligomers, polymers, and molecular crystals, with special qualities like a broad spectral absorption band and adjustable photophysical and photochemical characteristics, spurred research toward organic-based optoelectronic applications as a cost-effective substitute.

Brilliant green (BG) as a dye material is one of the other organic dyes, contains the $C_{27}H_{33}N_2.HO_4S$ Triarylmethane, a chemical compound used as a textile colorant, has the chemical formula HO_4S, which is one of its types. Additionally, it is employed in a number of vital electrical and optoelectronic devices, such as temperature sensors, photodetectors, electrochemical enzyme biosensors, and selective cut-off laser filters [1]. BG dye material for optoelectronic and nonlinear optic applications as an innovative device is previously reported [2].

Compared to inorganic semiconductors, which need to be coated on flat, unbending substrates, organic semiconductors are less brittle and provide several advantages, including as flexibility and low weight enabling easy movement. Organic semiconductors are generally easy to manufacture and conservative in research facilities. It is simple to create the red, green, and blue pixel matrix in organic semiconductor-based devices by inkjet printing or vacuum evaporation. Organic semiconductors have several uses in the field of optoelectronics for the creation of organic light-emitting diodes (OLED) and devices competing with LCDs, despite significant drawbacks, such as a shorter lifespan than that of conventional liquid crystal displays (LCDs). We have studied the dielectric response of BG based heterojunction using the characteristics of C-V and G-V at several frequencies.

Many electrical parameters can be determined by the use of impedance spectroscopy, a potent and well-known technique for analyzing the electrical properties and relaxation processes of semiconducting materials. Using established relations, the complex impedance Z, which is made up of an imaginary portion Z" and a real part Z', may be approximated from measured values of C-V and G-V characteristics.

Impedance spectroscopy is a powerful and well-known method for examining the electrical characteristics and relaxation processes of semiconducting materials. It may be used to determine a wide range of electrical parameters. The measured values of capacitance and conductance can be used to approximate the complex impedance Z, which is composed of an imaginary part Z" and a real part Z',

*Address correspondence to this author at the Film Device Fabrication–Characterization and Application FDFCA Research Group USTOMB, 31130, Oran, Algeria; E-mail: mostefa.benhaliliba@univ–usto.dz

using existing relations. A detailed investigation on the complex dielectric ε*, electric-modulus M*, impedance Z*, tangent-loss tanδ, and Ac conductivity (σ_{ac}) of the Al/(S:DLC)/p-Si/Au (MIS)-type Schottky structures in a large band of voltage and frequency is earlier achieved [3]. The Al/Al_2O_3/PVA voltage-dependent graphs of, ε″, tan δ, and σ_{ac} are mentioned in previous works. The n-ZnSe MIS diode is examined, displaying diagrams and interesting factors such as the impact of the thickness of the Al_2O_3 interfacial insulator layer between Al and PVA: n-ZnSe and capacitance of the insulator layer are investigated [4]. The observed frequency dispersion in the C–V and G/ω curves can be attributed to the interface states (Nss), series resistance (Rs), dielectric constant (ε'), dielectric loss (ε″), loss (tan δ), and Ac electrical conductivity (σ_{ac}) [4].

The metal semiconductor diode-based Ag:ZnO doped PVP interfacial layer showing dielectric response and related parameters is earlier studied by Yeriskin *et al*. [5]. The effects of applied voltage and frequency on the structural single relaxation process and dielectric properties are shown by means of Nyquist diagrams [5].

The impact of frequency variation on the dielectric properties of organic layers based on BODIPY dye is emphasized [6]. Oxide layers, organic compounds, insulators, etc. are employed as interfaces between metal and semiconductor to improve the performance of MS devices. The significance is how certain organic and polymer substances utilized in the interface affect the dielectric characteristics is discussed and considered. There has been prior research on the impact of TiO_2 nanoparticles on the barrier inhomogeneity of brilliant-blue fruit dye-base solar cells [7].

It is reported, that biocompatible Coomassie brilliant blue dye is produced on silicon based organic/Inorganic heterojunction for photodetection applications [8]. Photodetecting properties of Brilliant Blue-FCF implemented device for organic-based optoelectronic applications are revealed as mentioned elsewhere [9].

Here, using the measurements of capacitance and conductance versus voltage at several frequencies, we study the impedance spectroscopy of diode-based BG dye material. Several parameters are investigated as a result of frequency. It is demonstrated that capacitance, conductance, dielectric constant, and angle loss are depending on voltage and frequency.

Up to our best knowledge, there are no papers which reported on electronic device based on BG dye organic material, none their spectroscopy impedance study. We focus on impedance spectroscopy and dielectric response of heterojunction-based BG organic material. Our study is detailed to explore more behaviors of BG based heterojunction like electrical characteristics C/$_f$-V, G/$_f$-V, dielectric parameters, relaxation process, interfacial polarization, unique distribution of surface states in the band gap of semiconductors and dipole polarization.

2. EXPERIMENTAL SET UP

Getting high-quality electronic equipment requires cleaning. In order to remove any remaining grease and contaminants that have adhered to the substrate surface, the p-Si wafers doped with boron and having a resistivity of 1–10 Ωxcm are degreased in a boiling trichloroethylene solution for five minutes, then vibrated in acetone and methanol in an ultrasonic bath. In a hydrofluoric acid bath, the native oxide layers on the surface of silicon wafers are chemically erased. The procedure is finished right before the deposition to create a Si surface that is hydrogen-passivated, preventing the production of oxides while the substrate is being stored. Prior to making the device, the unpolished side of the Si wafer is thermally evaporated in a Nanovak NVBJ-300TH vacuum system at 10^{-6} torr using 200 nm high purity (4N) Al thick metal purchased from Kurt J. Lesker Company. The metal is then annealed in a furnace at 420°C for 3 minutes to obtain low resistive ohmic contact. The easy spin coating method is used in the production of the BG molecule-based gadget. We dilute 24 mg of BG (purchased from Sigma Aldrich) in 50 milliliters of methanol. BG thin films are applied to the p-Si substrates using a spin coater that spins for five minutes at 2000 rpm. These thin-film measurements yield a thickness of 673 nm at high frequencies through capacitance-voltage measurements.

A quantity of 24 mg of BG (purchased from Sigma Aldrich) is diluted in 50 milliliters of methanol. Such a thin layer has a thickness of 673 nm. Next, a 1.5 mm-diameter mask was used to evaporate high-purity Au metal, resulting in 200 nm Au front contact with the structure. Figure **1** depicts the cross-section of the Au/BG/p-Si/Al heterostructure, which displays the dye BG brilliant green chemical structure. The Agilent 16034 H impedance analyzer setup is used to measure the C-V ad G-V characteristics in a dark, room-temperature environment as drawn in Figure **1 B**-**C**. Figure **2** displays the facilities of thin film deposition like spin coating (A) and thermal evaporation (B).

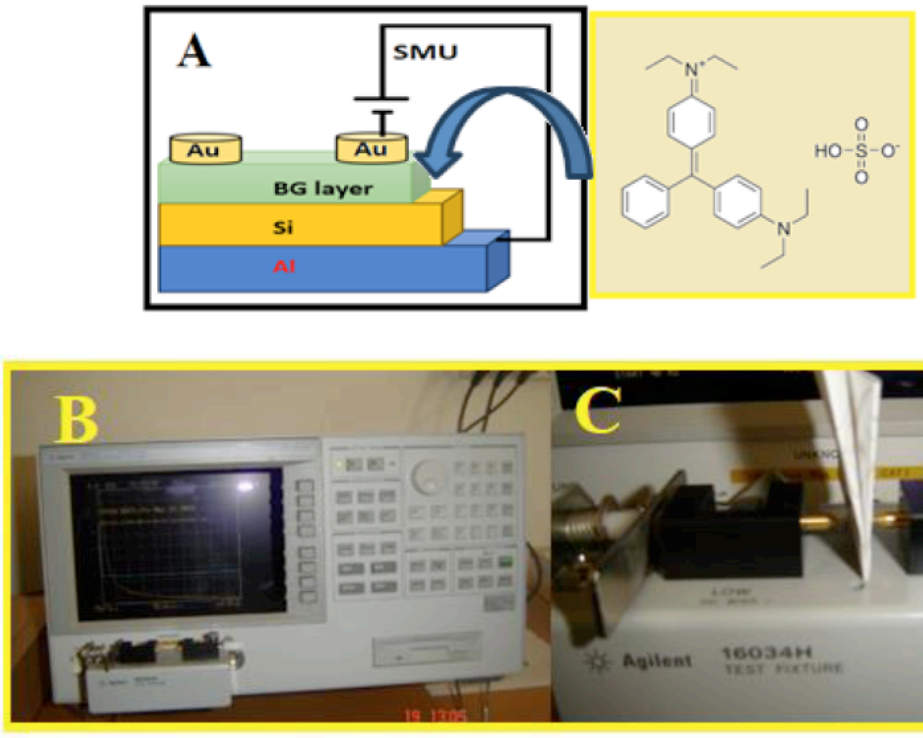

Figure 1: Architecture of Au/BG/Si/Al heterostructure (**A**), Impedance meter set-up (**B**), sample between contact for C-V measurement (**C**).

Figure 2: The facilities of thin film deposition: spin coating (**A**); thermal evaporation (**B**).

3. RESULTS AND DISCUSSIONS

3.1. Impedance Spectroscopy

At room temperature the capacitance-voltage characteristics of our electronic device based on BG dye material are plotted in Figure **3** for several applied frequencies (100,200, 500 kHz and 1MHz). It is clearly observed that almost no change of capacitance with frequency in reverse voltage and a slight evolution of C-V with bias. While a drastic growth of C-V from -0.23 V is observed within forward voltage for all frequencies as indicated by arrow in Figure **3 I**. Three regions are recorded in this plot, deep depletion (dd), depletion(d) and accumulation (a) for lower, medium and higher values of capacitance within reverse-forward (-2V, +2V) range.

The plot shows a scan of capacitance from 214 pF at -2V to 1 nF at +2V. As sketched in Figure **3 II**, the distinction between curves at various frequencies starts at -1.12 V, as indicated by a rectangle, recording a decline of capacitance with an increase of frequency. A discrepancy of (782-448) pF as a result of frequency values is observed in Figure **3 III**. It is often that C-V curves present an anomalous peak in forward region, in particular accumulation region, due to some behaviors like interfacial polarization, unique distribution of surface states in the band gap of semiconductors and dipole polarization as reported previously for MgPc organic layer-based heterojunction. The capacitance of the MgPc/GaAs organic diode is measured at two large peaks, about 20 nF and 70 nF, at 0.6 V and 3.25 V, respectively. A valley is also seen at the edge of depletion and deep depletion areas, at

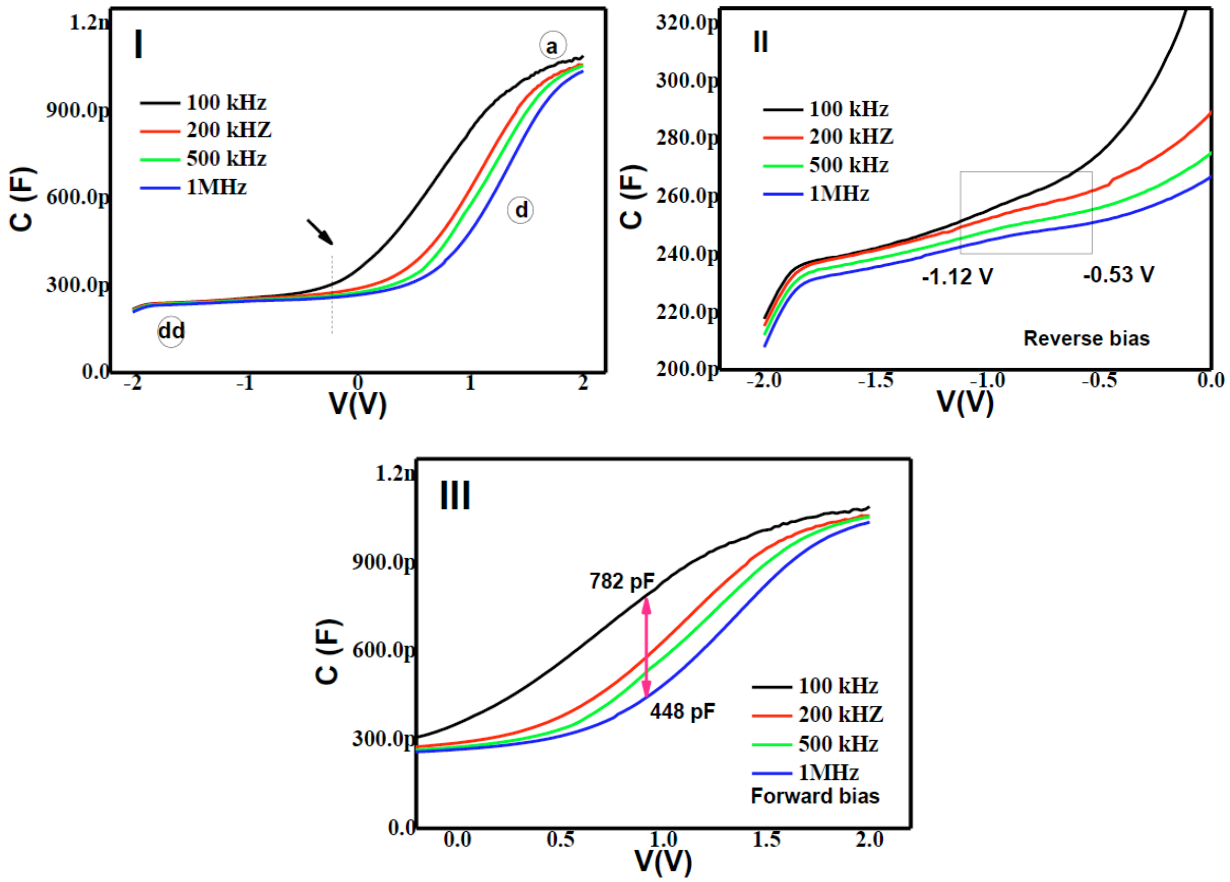

Figure 3: C-V characteristics of Au/BG/Si/Al heterostructure at different applied frequencies. I-C-V plot within -2V, 2V range, II-C-V in reverse bias, III- C-V in forward bias ranges.

around 1 V [10]. It' s not the case here, only a maximum is reached at accumulation region. This fact can be interpreted that dipoles in our BG based heterojunction have more time to turn in the same axis of electric Ac field. The dissipation factor or angle loss is expressed in terms of real and imaginary parts of dielectric constant by [10];

$$tan\delta = \frac{\varepsilon''}{\varepsilon'} = \frac{G}{\omega C} \quad (1)$$

where the ε' and ε" are the real and imaginary parts of dielectric constant ε. Where G, C and ω=2πf are the values of conductance, capacitance and frequency respectively.

Figure **4** displays the conductance parameter as a function of biasing voltage of Au/BG/Si/Al heterostructure at different applied frequencies. Almost no change of conductance values with frequency modification is observed within reverse bias but G-V curves are increasing drastically with frequency in forward voltage as shown by the rectangle in Figure **4**. It is observed that high values of conductance are recorded for high frequency. Almost, there is no conductance change with frequency within reverse bias voltage and the curves are discernibly separated with frequency as shown in Figure **4**. The conductance of Ag/MgPc/GaAs/Au-Ge organic heterojunction for 500 kHz-1 MHz range is strongly frequency dependent as reported previously [10].

The capacitance value of vacuum is given by [10, 11]

$$C_0 = \frac{\varepsilon_0 A}{d_i} \quad (2)$$

where ε_0 is the permittivity of vacuum (8.84×10^{-12} F/m), A is the contact area (0.071 cm^2) and d_i is the thickness of layer (673 nm). So, C_0 is found to be 93 pF. The dielectric constant ε' and ε" are written as follows [12];

$$\epsilon' = \frac{C}{C_0} \quad (3)$$

$$\varepsilon'' = \frac{G}{\omega C_0} \quad (4)$$

Figure **5** and **6** show the profile of ε' and ε" of Au/BG/Si/Al heterostructure against applied voltage for all experimental frequencies. It is concluded that dielectric constant and C-V curves obey to the same profile. The angle loss of our device at various frequencies is plotted in Figure **7**. An increase of angle loss is confirmed with a decline of frequency as seen within forward voltage.

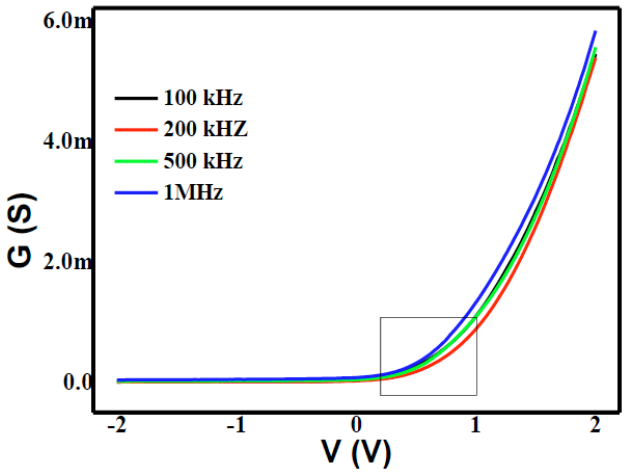

Figure 4: G-V characteristics of Au/BG/Si/Al heterostructure at different applied frequencies.

The Ni/PEDOT: PSS/CV/p-Si/Al diode is already studied and important findings are previously reported. Deniz *et al*. have highlighted that the C-V characteristics of diodes, evaluated at different frequencies at room temperature, exhibit a drop as the frequency value increases [13].

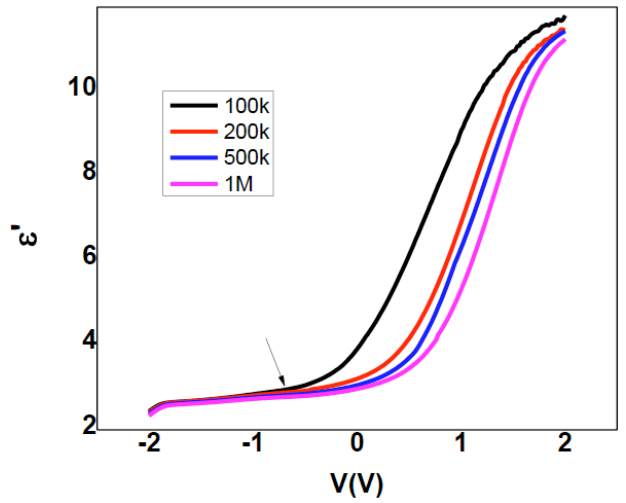

Figure 5: Real part of dielectric constant versus voltage of Au/BG/Si/Al heterojunction. Effect of frequency starts where arrow indicates

It is noted that dipoles do not have enough time to orient themselves in the high frequency electric field are the cause of the drop in ε ′ and ε ″ within the forward voltage zone as depicted in Figures **5** and **6**. The ε’ curve also produces the relaxation peaks like C–V plot because the dipoles may turn around their axis in the direction of the electric field and have enough time to follow the frequency of the Ac signal at low frequencies. Similar explanation is reported for CdS-PVA/Si heterojunction [14]. Dielectric processes usually include electronic, ionic, dipole, and interfacial polarization, and whereas the first two of these can occur at very high frequencies, for f>> 1GHz, the latter can occur at lower frequency as is interpreted earlier [14].

These mechanisms, which have to do with the relaxation process, may make it easier for an interfacial layer to polarize when there is an electric field present at low frequencies. The rising of ε′ and ε″ with decreasing frequency in the depletion area can also be attributed to the traps, which have the ability to store and release electrons in the presence of an external electric field [15].

3.2. Electrical Modulus

In addition to impedance analysis, modulus analysis is a powerful technique for researching deeper into the subject matter and providing a clearer picture and a more thorough explanation of the electrical principles at work. The capacity to distinguish between various relaxation mechanisms arising in grains, grain borders, and grain electrode interfaces is the excellence of modulus spectroscopy. Unlike impedance spectroscopy, modulus spectroscopy examines the area with the least capacitance while ignoring electrode contributions. This allows one to discern the individual effects of each nanostructure on the film overall electrical behavior.

The influence of electrode polarization and carrier charge transfer, which can result in inaccurate (high values of permittivity and conductivity), particularly at high temperatures, was eliminated using the electric modulus formalism. As an electrical counterpart of the mechanical shear modulus, reciprocal complex permittivity was examined, and the electric modulus approach got underway.

The complex electric modulus M* expresses as [10, 16];

$$M^* = \frac{1}{\varepsilon^*} = \frac{\varepsilon' + j\varepsilon''}{\varepsilon'^2 + \varepsilon''^2} \quad (5)$$

The real and imaginary components of M* are written as [10];

$$M^* = M' + jM'' = R_s + j\frac{1}{\omega C_s} \quad (6)$$

where real M’ and imaginary M” parts of modulus M* are expressed as [17];

$$M' = \frac{\epsilon'}{\epsilon'^2 + \varepsilon''^2} = C_0\left(\frac{\omega^2 C}{\omega^2 C^2 + G^2}\right) \quad (7)$$

$$M'' = \frac{\epsilon''}{\epsilon'^2 + \varepsilon''^2} = C_0\left(\frac{\omega G}{\omega^2 C^2 + G^2}\right) \quad (8)$$

where C is the measured capacitance, G is the measured conductance, $\omega = 2\pi f$ is the angular frequency of the applied Ac field. Resistance R in terms of dielectric constant is expressed as [10];

$$\frac{1}{R} = \frac{\varepsilon''}{\varepsilon_0} C_0 \omega \quad (9)$$

It is well known that dielectric materials—such as insulators, ferroelectrics, and pure or dopant polymers/organics—polarize readily in the presence of an external electric field. When carriers have enough time, this polarizing effect causes them to circle around themselves and shift from one trap to another. Stated otherwise, an excess dielectric constant is created in relation to the actual parameter value when relaxation time causes the dielectric parameters to fluctuate with the applied electric field and frequency, especially at low and moderate frequencies. In literature, M/S-doped DLC/S (MIS) type Schottky-structures diodes present a decline of M' with increase in voltage and peaks presence in M" curve [18].

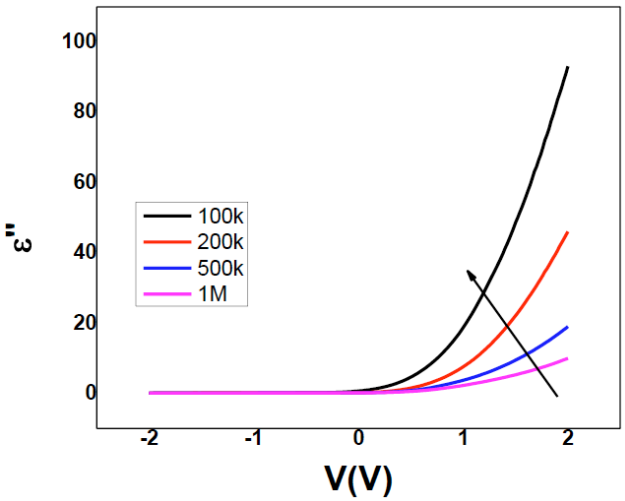

Figure 6: Imaginary part of dielectric constant ε" versus voltage of Au/BG/Si/Al heterojunction. The arrow indicates the increase of ε" with a decline of frequency.

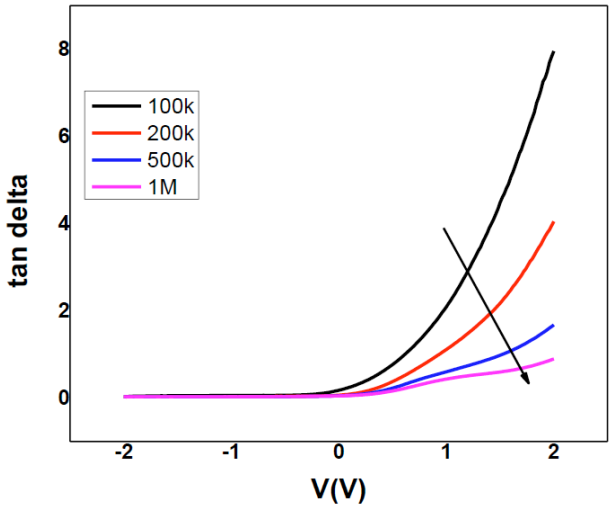

Figure 7: Angle loss parameter versus voltage of Au/BG/Si/Al heterojunction. Angle loss decreases with an increase of frequency as shown by arrow.

Real M' and imaginary M" components of modulus parameter of Au/BG/Si/Al are plotted within -2V, +2V range for 100, 200, 500 kHz and 1MHz as shown in Figures **8** and **9**. A lowering of M' is sketched from reverse to forward voltage range but a gaussian profile of M" recording a peak within 0.5-1 V range is revealed. M" curve of MgPc/GaAs organic heterojunction demonstrates two peaks for all frequencies inside reverse voltage range as reported previously [10].

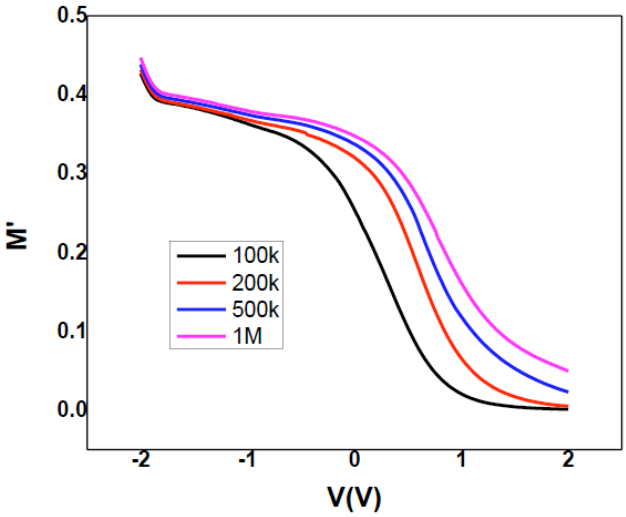

Figure 8: Real part of modulus parameter versus voltage of Au/BG/Si/Al heterojunction.

The Complex impedance Z*, real Z* (Z') and Im Z* (Z") are written as [19, 20];

$$Z^* = \frac{1}{j\omega C_0 \varepsilon^*} \quad (10)$$

$$Z' = \frac{\varepsilon''}{\omega C_0 (\varepsilon'^2 + \varepsilon''^2)} \quad (11)$$

$$Z'' = \frac{\varepsilon'}{\omega C_0 (\varepsilon'^2 + \varepsilon''^2)} \quad (12)$$

It is earlier reported that real part of M' of MgPc/GaAs organic device at 500, 700 kHz and 1 MHz demonstrates a similar decay within the reverse bias (-2V, 0.5 V) range.

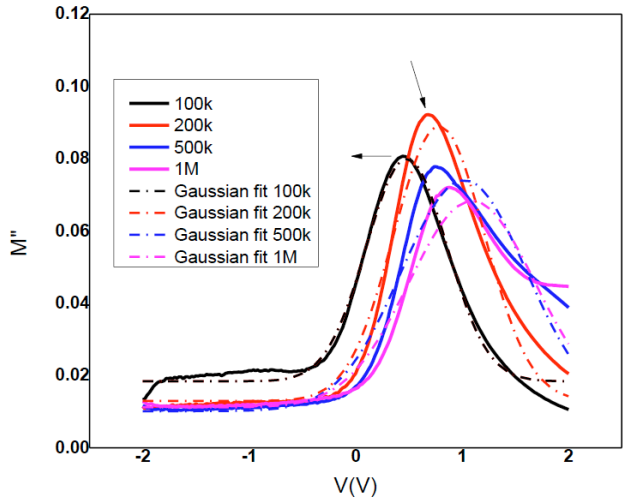

Figure 9a: Imaginary part of modulus parameter versus voltage of Au/BG/Si/Al heterojunction. Peaks of M" are shown by arrows and peak shift as a result of frequency is indicated by arrow.

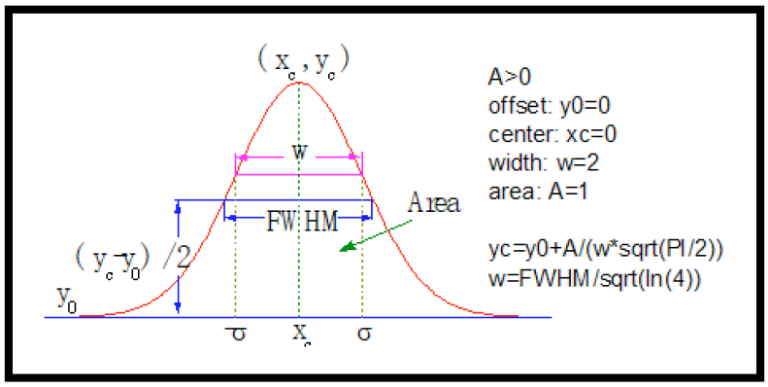

Figure 9b: Gaussian fit curve and related parameters.

The real and imaginary components of Dc conductivity are written as [10];

$$\sigma' = \omega\epsilon_0\epsilon'', \sigma'' = \omega\epsilon_0\epsilon' \quad (13)$$

The M'' profile of MgPc/GaAs organic heterojunction for following frequencies 500, 700 kHz and 1 MHz presents approximately a similar curve showing a peak in the forward voltage range for all applied frequencies [10]. Figure **7** reveals that the M' values are commonly lowering with an increasing voltage; though, M"- V curves exhibit peaks for each frequency as depicted in Figure **9a**. Specifically, the position of the peak is shifted from low to high voltage within forward bias voltage when frequency increases as listed in Table **1**. The position of peak is spotted by xc value given by the gaussian fit. The value of xc is increasing from 0.48 V to 1.09 V with frequency as demonstrated in Table **1**. These values confirm the experimental findings discussed above related to Figure **9**. The width of M"-V peak curve is enlarged by increase of frequency as indicated in Figure **9** and in Table **1**. Such results might due to surface states, relaxation times, and Maxwell-Wagner polarization and the obtained results are in well agreement with previous works [21, 22].

The phase angle as a function of Z' and Z" is written as [23];

$$\theta = tan^{-1}\left(\frac{Z''}{Z'}\right) \quad (14)$$

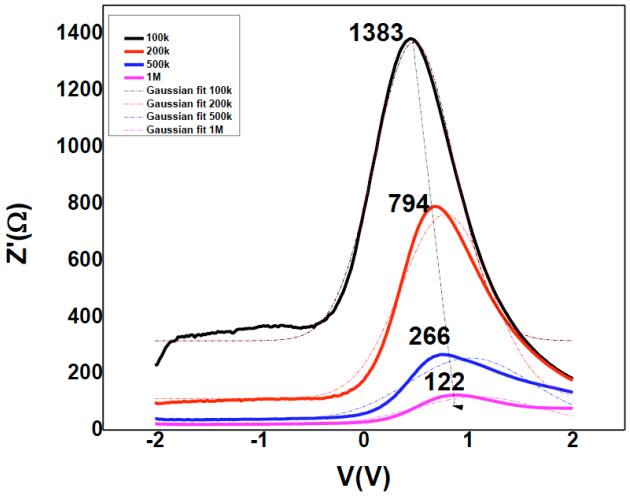

Figure 10: Real part of complex impedance Z' parameter versus voltage of Au/BG/Si/Al heterojunction. Peak values are displayed and dashed curve shows a peak shift of Z'.

The curves Z'-V of our device-based BG present a peak of 1383 Ω and becomes more broadened and less intense and shifts to higher voltage values when frequency increases as shown in Figure **10**. It is revealed that highest peak is 1383 Ω at 100 kHz then declines to 122 Ω for 1MHz recording a shift towards high voltage as indicated by dashed curve in Figure **10**. A gaussian fit is plotted for all frequencies as seen in Z'-V curve. As showed in Table **2**, intensity of peak is given by height (Ω), which is a little bit than Z' values, ~1054-97 Ω, but peak width is increasing with frequency and shifted to higher voltage as assigned by

Table 1: Obtained Parameters from Gaussian fit of M"-V curve of Heterojunction Based Organic BG Dye Layer. Gaussian Equation used for fit is $y=y_0+ A*exp^{-2(x-xc)2/w2}/w(\pi/2)^{0.5}$. y_0 is Intercept, xc Abscissa of Peak, w is the Peak Width, FWMH is Full Width at Medium Height. Details are Displayed in Figure 9b.

f (Hz)	y_0	xc (V)	FWMH (V)	Height	w (V)
100k	0.018	0.48	0.89	0.06	0.75
200k	0.013	0.78	1.00	0.08	0.85
500k	0.010	1.02	1.38	0.06	1.17
1M	0.011	1.09	1.39	0.06	1.18

Table 2: Obtained Parameters from Gaussian fit of Z'-V Curve of Heterojunction Based Organic BG Dye Layer. Gaussian Equation used for fit is $y=y_0+ A*exp^{-2(x-xc)2/w2}/w(\pi/2)^{0.5}$. y_0 is Intercept, x_c Abscissa of Peak, w is the Peak Width, FWMH is full Width at Medium Height

f (Hz)	y_0 (Ω)	xc (V)	FWMH (V)	Height (Ω)	w (V)
100k	314.97	0.48	0.89	1054.3	0.76
200k	111.00	0.78	1.00	650.8	0.85
500k	34.72	1.02	1.38	218.98	1.17
1M	19.19	1.09	1.39	97.82	1.18

xc data. The two bands, 1383-122 Ω and 1054-97 Ω, are roughly adjacent to one another.

While imaginary part (Z") of Z depicts a decay from 7328 Ω at -2V to lower value at +2V as portrayed in Figure **11**. It is recorded that the highest values of Z' and Z" are obtained for 100 kHz and Z" values are in order of 5 times of that of Z' approximately. Particularly at low frequencies, the forward biasing voltage frequency is independent of the impedance values, and every one of the curves combine together. Similar behaviors are previously recorded as M/S-doped DLC/S diode which exhibits an increase in Z' plot with a decrease in frequency from 2 M to 2 kHz showing peaks within reverse voltage range. A value of Z' exceeding $2x10^5$ Ω is reported whereas a decline of Z" is recorded from reverse to forward voltage range. An abrupt fall of Z" from 0 V, in particular 0-1 V range, which corresponds to the depletion region. This drastic decay is seen for lower frequency (100 and 200 kHz) and Z" values become constant beyond 1V for the used work frequencies. Consequently, both Z' and Z" values are frequency dependent.

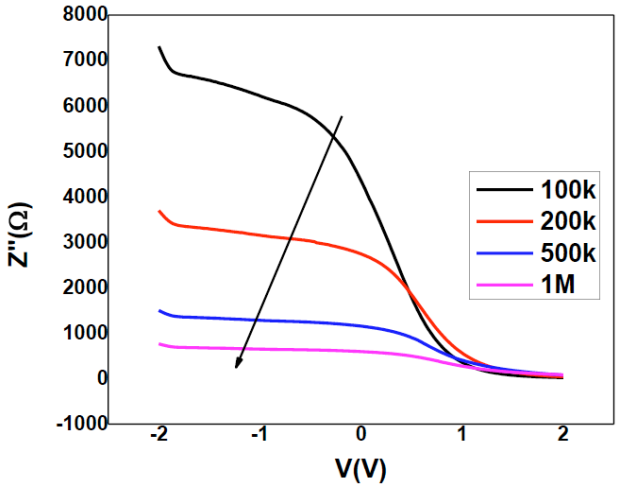

Figure 11: Imaginary part of complex impedance Z" parameter versus voltage of Au/BG/Si/Al heterojunction. Z" is lowering with an increase of frequency as displayed by arrow.

In order to reduce technological challenges in both organic and inorganic semiconductor devices and connections, silicon is frequently chosen as the substrate. Deposition of organic materials (dyes, pigments, and metal complexes) on top of the inorganic

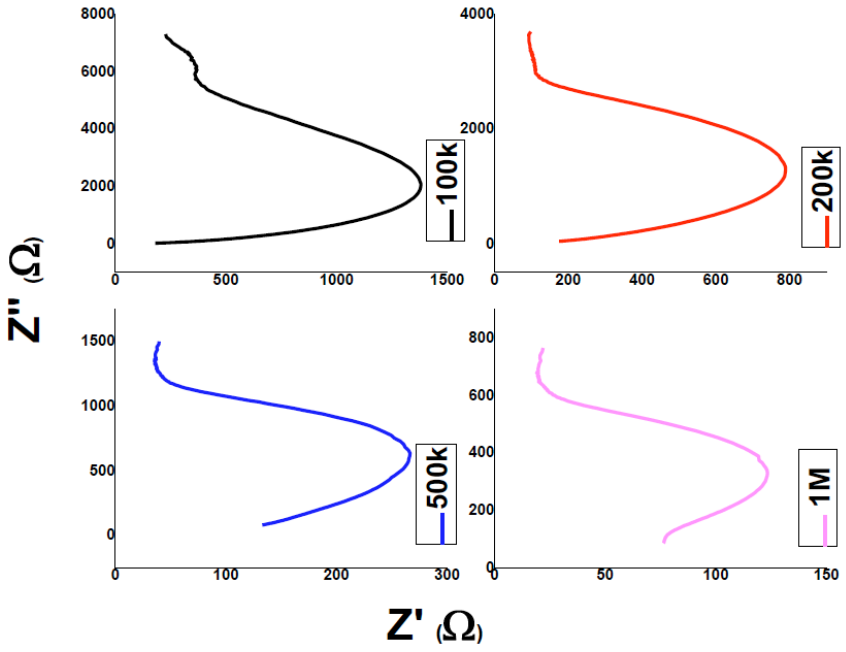

Figure 12: Nyquist diagram of Au/BG/Si/Al heterojunction for several frequency curves.

semiconductor substrate in this designed device can create a large number of interface states on the surface of the semiconductor substrate and alter the junction diode characteristics as mentioned by Güllü *et al*. [24]. Our Au/BG/p-Si/Al Schottky diode has a low-resistivity layer and a highly resistive layer, meaning it has its own capacitance. An oxide layer between the BG layer and p-Si may form during the silicon substrate cleaning process, which might potentially have an impact on the capacitance profile of the device under study.

Au/pyronin-Y/p-Si/ Al Schottky diode revealed similar peaks and records of 15 kΩ at lowest frequency of 2 kHz and declines with an increase of frequency [25].

Plotting of the Nyquist diagram displays single semicircular arcs with varying sizes according on the applied Ac signal frequency. The findings of the morphological structural study in BG are validated by these semicircles. Thus, the semicircle radius falls with an increasing applied frequency.

It is possible to discuss features like the relaxation time, resistance, conductivity, and capacity since the radius of each semicircle is connected to the constructed device resistance and Ac conductivity. Both the conductivity and the resistance decrease with a decreasing radius. Figure **12** sketches the Nyquist diagram of organic heterojunction-based BG dye material. This figure makes it clear that the Z" vs. Z'

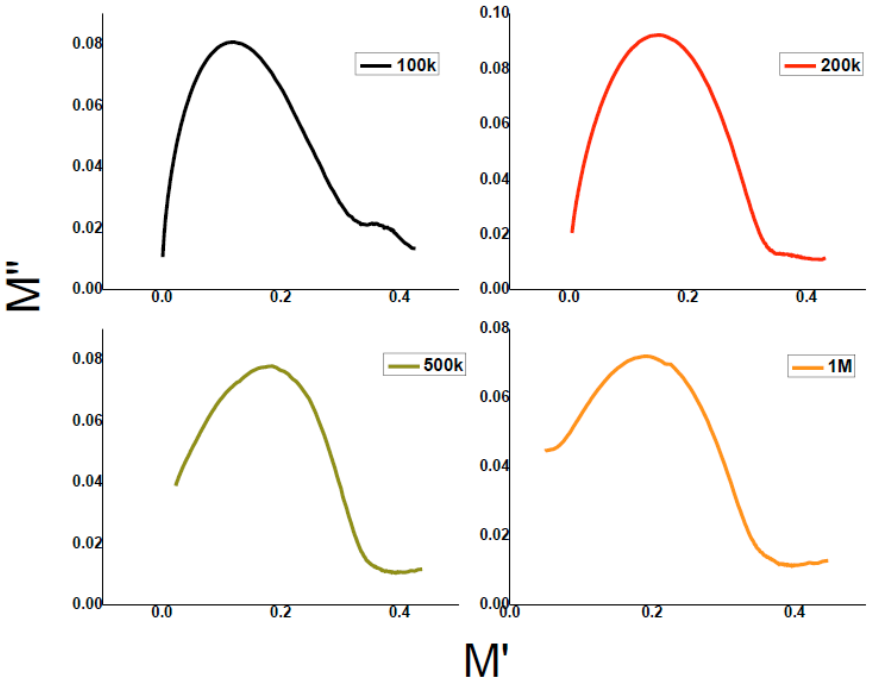

M"-M' curves for various frequencies of our device are plotted in Figure **13**. A peak occurrence is observed within 0-0.2 range of M'.

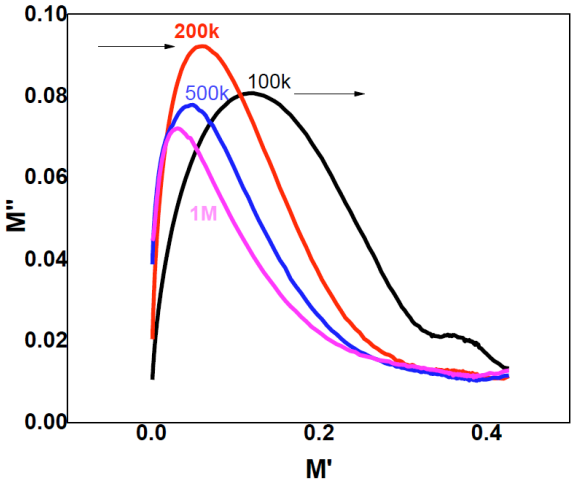

Figure 13: M"-M' diagram of Au/BG/Si/Al heterojunction. Each curve is identified by its frequency and peak shift is indicated by arrow.

curves have a clear peak or semicircular shape at all frequencies, with the peak value rapidly dropping as the frequency rises. Based on the Z' axis, the observed semicircle and its radius are selected for four distinct frequencies. The observed behavior clarifies how polarization or relaxation processes rapidly decrease with rising frequency. The curves show that frequency affects significantly the dielectric characteristics. Furthermore, peak of Z" value diminishes with frequency increase. Similar curves of Z"-Z' are prior shaped for DLC/S (MIS type) structure [18].

The electrical conductivity real part σ' and imaginary σ" are plotted in Figures **14** and **15** showing an increase of curves from reverse to forward bias voltage. Here contrary to Z' and Z", the conductivity increases with an increase of frequency.

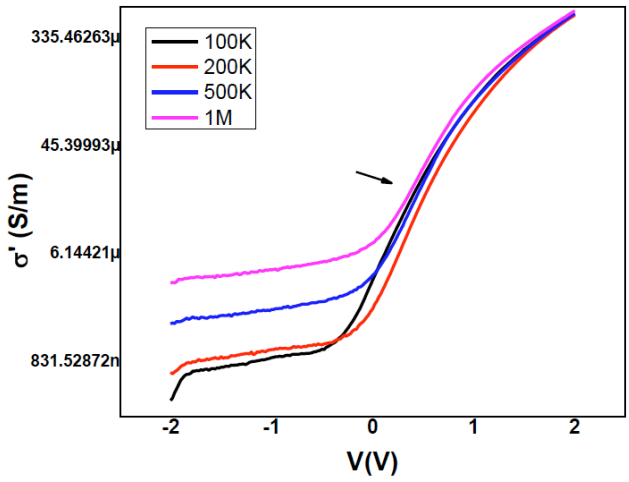

Figure 14: Semilog Real part of conductivity versus voltage of Au/BG/Si/Al heterojunction. Effect of frequency on σ' is displayed as arrow indicates.

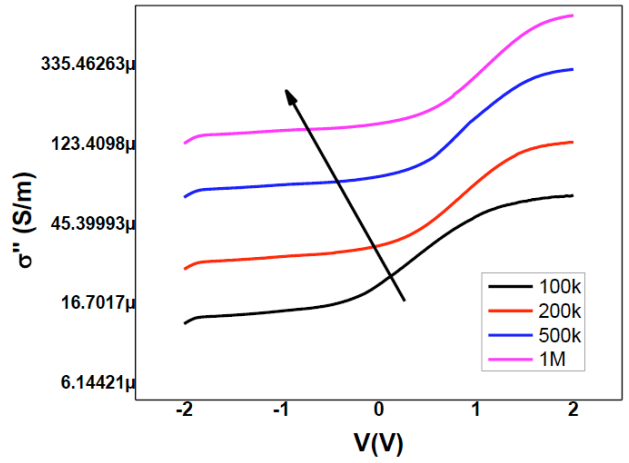

Figure 15: The semilog Imaginary part of conductivity versus voltage of Au/BG/Si/Al heterojunction. Increase of σ" with frequency is shown by arrow.

Both σ' and σ" curves present a growth with frequency from reverse to forward voltage range. Here, the parameter σ' attains a highest value of 5.53×10^{-4} S/m at 1 MHz but 6.18×10^{-4} S/m is the highest point reached by σ". Similar trends are earlier reported for MgPc film based organic heterojunction but conductivity values are so smaller [10]. Ac conductivity of Au/BODIPY/p-Si devices at various frequencies (100-1000 kHz) present similar growth from reverse to forward bias voltage as mentioned previously [6]. The highest obtained values of Au/BODIPY/p-Si is comprised between 4×10^{-7}-5×10^{-7} S/m. At lower frequency, the conductivity is found to be frequency independent in the low frequency (Dc plateau) which rises with the increase of the frequency as indicated in previous work [26].

Generally, the Jonscher power law explains the conductivity dispersion mechanism [10, 27] as;

$$\sigma = \sigma_{dc} + A\omega^n \quad (15)$$

where σ_{dc} (~σ") is the frequency independent Dc part of Ac conductivity (~σ') in the low frequency area, ω is the angular frequency, n is frequency exponent related to charges and A is a constant. Specifically, in the upper frequency range (1MHz), it is evident that the decrease in interfacial polarization causes the value of σ_{ac} to increase with frequency. The energy loss tanδ is the result of the current increasing due to the growth in σ_{ac}. As previously observed [10], the cause of σ_{ac} occurrence is the decrease in series resistance (Rs). It turned out that the conductivity displays a thermally activated characteristic [28] in accordance with the conductivity value at 100 Hz, as mentioned previously [26].

This result is often interpreted by Arrhenius law, $\sigma=\sigma_0 \exp^{-Ea/k_B T}$, where σ_0 is pre-exponential factor and Ea is the activation energy related with the conduction process. This energy is extracted by the slope of $\ln\sigma_{dc}$ vs. $10^4/T$ as cited prior [26].

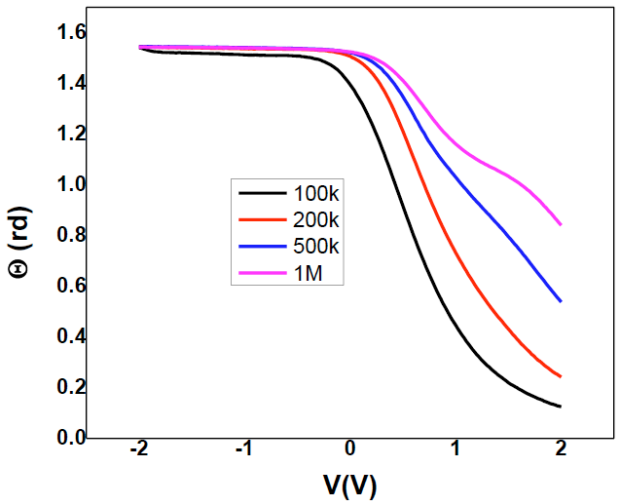

Figure 16: Angle phase versus bias voltage of Au/BG/Si/Al for several frequency curves.

The frequency dependence of angle phase of BG based heterojunction at various frequencies is presented in Figure **16**. No effect of frequency on angle phase is occurred within reverse bias but a strong decay is confirmed within forward bias as portrayed in Figure **16**.

Angle phase is still constant around 88º within reverse voltage which reveals a capacitive conduct.

Such behavior occurring in the interfacial layer can be well-defined by the phase angle, which reaches minor values around zero at low frequencies as reported before [3].

CONCLUSION

Throughout this research, a complete study of dielectric response and impedance spectroscopy of Au/BG/Si/Al for several frequencies is achieved. Voltage and frequency dependent capacitance, conductance, dielectric constant, angle loss are evidenced. The results of the experiment show that a variety of factors affect the dielectric characteristics, M', M", and Ac conductivity of BG organic structures. These factors include interlayers between the interface, their thickness, polarization processes, hopping mechanisms, interface states/traps, their frequency and voltage.

Our device-based BG exhibits the peak at 1383 Ω as seen in Z'-V curve, then as frequency rises, they expand, become less intense, and gain a transition to higher voltage levels. Intensity of peak presence in Z'-V plot is lowering with increase in frequency and a shift to higher bias voltage is recorded. While Z''-V curve are decreasing from reverse to forward voltage range

M"-M' plots show a broadened peak for each frequency and recorded value is comprised between 0.08 and 0.1. M"-M' curves are strongly frequency dependent.

Nyquist diagram of Au/BG/Si/Al heterojunction for several frequency curves is sketched recording semicircular shape of Z"-Z' curve. These semicircles support the results of the morphological structural investigation in BG. With an increase in applied frequency, the semicircle radius decreases.

It is noted that our device exhibits lower conductivity which is increasing with frequency.

Within reverse bias voltage range, angle phase is still constant around 90º which reveals a capacitive conduct.

ACKNOWLEDGMENT

The research is included in the PRFU project under contract number N° B00L02UN310220220001 Oran University of sciences and technology USTO-MB. www.mesrs.dz, and www.univ-usto.dz. http://www.prfu-mesrs.dz/.
https://www.mendeley.com/impact/mostefa-benhaliliba, https://orcid.org/0000-0001-6507-3663 17

CREDIT AUTHORSHIP CONTRIBUTION STATEMENT

M. Benhaliliba: Methodology, Investigation, Visualization, Writing - review & editing.

A, Ayeshamariam: Methodology, Conceptualization, measurements, Investigation.

CE Benouis: improvement and discussions.

YS Ocak: discussion of results.

CONFLICT OF INTEREST

The authors declare that they have no conflict of interest

DECLARATION OF COMPETING INTEREST

The authors declare that they have no known competing financial interests or personal relationships that could have appeared to influence the work reported in this paper.

DATA AVAILABILITY

No data was used for the research described in the article.

REFERENCES

[1] Gonamanda Satya Sree, Sathish Mohan Botsa, Boggu Jagan Mohan Reddy, Kapilavayi Venkata Basava Ranjitha, Enhanced UV-Visible triggered photocatalytic degradation of Brilliant green by reduced graphene oxide based NiO and CuO ternary nanocomposite and their antimicrobial activity, Arpabian Journal of Chemistry, 13, 4 (2020) 5137-5150. https://doi.org/10.1016/j.arabjc.2020.02.012

[2] M. Benhaliliba, A. Ben Ahmed, Innovative Device Based Brilliant Green Dye Material for Optoelectronic and Nonlinear Optic Applications, Chemistry Africa.

[3] A Eroğlu Tezcan, S. A. Hameed, A Feizollahi Vahid, M Ulusoy, Ş. Altındal, A study on the complex dielectric (ε*)/electric-modulus (M*)/impedance (Z*), tangent-loss (tanδ), and ac conductivity (σac) of the Al/(S:DLC)/p-Si/Au (MIS)-type Schottky structures in a wide range of frequency and voltage at room temperature (RT), Physica B: Physics of Condensed Matter.

[4] Mamta Sharma, S.K. Tripathi, Frequency and voltage dependence of admittance characteristics of Al/Al2O3/PVA:n-ZnSe Schottky barrier diodes, Materials Science in Semiconductor Processing 41 (2016) 155-161. https://doi.org/10.1016/j.mssp.2015.07.028

[5] Seçkin Altındal Yeriskin, Esra Erbilen Tanrıkulu, Murat Ulusoy Dielectric properties of MS diodes with Ag:ZnO doped PVP interfacial layer depending on voltage and frequency, Materials Chemistry and Physics 303 (2023) 127788. https://doi.org/10.1016/j.matchemphys.2023.127788

[6] Lütfi Bilal Tasyürek, The effects of frequency change on dielectric characteristics in dye-based organic layers, Optik - International Journal for Light and Electron Optics 260 (2022)

169064.
https://doi.org/10.1016/j.ijleo.2022.169064

[7] Arnab Kanti Karan, Dipankar Sahoo, Nabin Baran Manik Investigating the effects of TiO2 nanoparticles on the barrier inhomogeneity of brilliant-blue fruit dye-base solar cell, Current Applied Physics 59 (2024) 95-104.
https://doi.org/10.1016/j.cap.2023.12.009

[8] Marwa S. Salem, Ahmed R. Wassel, M. Fedawy, A. Shaker, Amal H. Al-Bagawia, Ghada Mohamed Aleid, Ahmed M. El-Mahalawy, Integration of biocompatible Coomassie Brilliant Blue dye on silicon in organic/Inorganic heterojunction for photodetection applications Journal of Physics and Chemistry of Solids 169 (2022) 110890.
https://doi.org/10.1016/j.jpcs.2022.110890

[9] Othman Haji Mahmood, Ali Ugur, Arife Gencer Imer, The photodetection characteristics of a Brilliant Blue-FCF implemented device for organic-based optoelectronic applications, Journal of Physics and Chemistry of Solids 184 (2024) 111733.
https://doi.org/10.1016/j.jpcs.2023.111733

[10] M. Benhaliliba, T. Asar, I. Missoum, Y.S. Ocak, S. Özçelik, C.E. Benouis, A. Arrar, Ac Conductivity and Impedance Spectroscopy Study and Dielectric Response of MgPc/GaAs Organic Heterojunction for Solar Energy Application, Physica B: Condensed Matter Physica B: Condensed Matter, 578 (2020), 411782.
https://doi.org/10.1016/j.physb.2019.411782

[11] B. Chatterjee, N. Kulshrestha, P.N. Gupta, Nano composite solid polymer electrolytes based on biodegradable polymers starch and poly vinyl alcohol, Measurement 82 (2016) 490-499.
https://doi.org/10.1016/j.measurement.2016.01.022

[12] E. E Tanrıkulu, D.E. Yıldız, A. Günen, S. Altındal, Frequency and voltage dependence of electric and dielectric properties of Au/TiO2/n-4H-SiC (metal-insulator-semiconductor) type Schottky barrier diodes, Phys. Scripta 90 (2015), 095801.
https://doi.org/10.1088/0031-8949/90/9/095801

[13] A.R. Deniz, A.I. Tas, Z. Çaldıran Ü. Incekara, M. Biber, S. Aydogan, A. Türüt, Effects of PEDOT:PSS and crystal violet interface layers on current-voltage performance of Schottky barrier diodes as a function of temperature and variation of diode capacitance with frequency, Current Applied Physics 39 (2022) 173-182.
https://doi.org/10.1016/j.cap.2022.03.017

[14] Y. Azizian-Kalandaragh, I. Yücedag, G. Ersoz Demir, S. Altındal, Investigation of the variation of dielectric properties by applying frequency and voltage to Al/(CdS-PVA)/p-Si structures, J. Mol. Struct. 1224 (2021), 12.
https://doi.org/10.1016/j.molstruc.2020.129325

[15] S. Yasufuku, T. Umemura, Y. Ishioka, T. Tanii, Maxwell-wagner dielectric polarization in polypropylene film/aromatic dielectric fluid system for high voltage capacitor use, IEEE Transactions on Electrical Insulation, EI-14, Issue: 6 (1979).
https://doi.org/10.1109/TEI.1979.298189

[16] Irmak Karaduman Er, Ali Orkun Cagırtekin, Ahmad Ajjaq, Mem*et al*i Yıldırım , Aytun¸ Ates , and Selim Acar Complex electrical impedance and modulus characterizations of ZnO:Sn thin films in a wide temperature range, J Mater Sci: Mater Electron, May 2021.

[17] N. Delen, S. Altındal Yeris¸ kin, A. Ozbay, I. Tasçıoglu, Origin of frequency and voltage dependent negative dielectric properties in the Al/p-Si Schottky diodes with (Cd0.3Zn0.7O) interfacial layer in the wide range of frequency and voltage, Physica B 665 (2023) 415031.
https://doi.org/10.1016/j.physb.2023.415031

[18] A Eroğlu Tezcan, S. A. Hameed, A Feizollahi Vahid, M Ulusoy, Ş. Altındal, A study on the complex dielectric (ε*)/electric-modulus (M*)/impedance (Z*), tangent-loss (tanδ), and ac conductivity (σac) of the Al/(S:DLC)/p-Si/Au (MIS)-type Schottky structures in a wide range of frequency and voltage at room temperature (RT), Physica B: Physics of Condensed Matter.

[19] Demirezen, S.A. Yeris kin, Frequency and voltage-dependent dielectric spectroscopy characterization of Al/(Coumarin-PVA)/p-Si structures, J. Mater. Sci. Mater. Electron. 32 (2021) 25339-25349.
https://doi.org/10.1007/s10854-021-06993-1

[20] A.M. Akbas, A. Tataroglu, S. Altındal, Y. Azizian-Kalandaragh, Frequency dependence of the dielectric properties of Au/(NG:PVP)/n-Si structures, J. Mater. Sci. Mater. Electron. 32 (2021) 7657-7670.
https://doi.org/10.1007/s10854-021-05482-9

[21] Ö. Berkün, M. Ulusoy, Ş. Altındal, B. Avar, On frequency and voltage dependent physical characteristics and interface states characterization of the metal semiconductor (MS) structures with (Ti: DLC) interlayer, Physica B: Condensed Matter 666 (2023) 415099.
https://doi.org/10.1016/j.physb.2023.415099

[22] M. Shaban, A. Zkrıa, T. Yoshıtake, Temperature-Dependent Impedance Spectra of Nitrogen-Doped Ultra nanocrystalline Diamond Films Grown on Si Substrates, 9 (2021) 896-904.
https://doi.org/10.1109/ACCESS.2020.3046969

[23] M. Gokçen, H. Altuntas¸ S. Altındal, S. Ozçelik, Frequency and voltage dependence of negative capacitance in Au/SiO2/n-GaAs structures, Mater. Sci. Semicond. Process. 15 (2012) 41-46.
https://doi.org/10.1016/j.mssp.2011.08.001

[24] Ö. Güllü, Ş. Aydoğan, A. Türüt, Fabrication and electrical characteristics of Schottky diode based on organic materia lMicroelectronic Engineering 85, Issue 7(2008) 1647-1651.
https://doi.org/10.1016/j.mee.2008.04.003

[25] I.S. Yahia, H.Y. Zahran, F.H. Alamri, M. Aslam Manthrammel, S. Al Faify, Atif Mossad Ali, Microelectronic properties of the organic Schottky diode with pyronin-Y: Admittance spectroscopy, and negative capacitance, Physica B: Condensed Matter 543, (2018) 46-53.
https://doi.org/10.1016/j.physb.2018.05.011

[26] Saida Fatma Cherif, Amira Cherif, Wassim Dridi, Mohamed Faouzi Zid, Ac conductivity, electric modulus analysis, dielectric behavior and Bond Valence Sum analysis of Na3Nb4As3O19 compound Arabian Journal of Chemistry, 13, issue 6 (2020) 5627-5638.
https://doi.org/10.1016/j.arabjc.2020.04.003

[27] Andrew K Jonscher, 1999 J. Phys. D: Appl. Phys. 32 R57.
https://doi.org/10.1088/0022-3727/32/14/201

[28] Khan, G.A., Hogarth, C.A., 1991. The behaviour of SiOx/SnO thin dielectric films in an alternating electric field. J. Mater. Sci. 26, 17- 22.
https://doi.org/10.1007/BF00576026

Received on 03-09-2024 Accepted on 11-10-2024 Published on 15-10-2024

https://doi.org/10.31875/2409-9694.2024.11.06